Supporting information for:

Ligand discovery for a peptide-binding GPCR by structure-based screening of fragment- and lead-like chemical libraries

Anirudh Ranganathan[1,§], Philipp Heine[2,§], Axel Rudling[1], Andreas Plückthun[2,*], Lutz Kummer[2,3], Jens Carlsson[4,*]

[1] Science for Life Laboratory, Department of Biochemistry and Biophysics, Stockholm University, SE-106 91 Stockholm, Sweden.
[2] Department of Biochemistry, University of Zurich, Winterthurerstrasse 190, 8057 Zurich, Switzerland.
[3] G7 Therapeutics AG, Grabenstrasse 11a, 8952 Schlieren, Switzerland.
[4] Science for Life Laboratory, Department of Cell and Molecular Biology, Uppsala University, BMC, Box 596, SE-751 24 Uppsala, Sweden.

[§] These authors contributed equally to this work.

Keywords: fragment-based lead discovery, G protein-coupled receptor, drug design, molecular docking, virtual screening

Supporting methods

Molecular docking screening. All docking calculations were carried out with the program DOCK3.6[1] against a high-resolution crystal structure of NTSR1 (PDB accession code: 4BUO)[2]. Unless stated otherwise, the protonation states of ionizable residues Asp, Glu, Arg, and Lys in the binding site were set to their most probable states in the receptor at pH 7. Histidine tautomeric states were set by visual inspection on the basis of the hydrogen bonding network. His132$^{2.69}$ and His348$^{7.32}$, which are located in the NTSR1 binding site, were both protonated in the Nδ position. The flexible ligand sampling algorithm in DOCK3.6[1] superimposes atoms of the docked molecule onto binding site matching spheres, which indicate putative ligand atom positions. A total of 66 matching spheres were used and were based on residues 11-13 of NTS8-13. The spheres were also labeled for chemical matching based on the local receptor environment[3]. The degree of ligand sampling was determined by the bin size, bin size overlap, and distance tolerance. These three parameters were set to 0.4 Å, 0.1 Å (fragment library) or 0.2 Å (lead-like library), and 1.5 Å, respectively, for both the binding site matching spheres and the docked molecules. For ligand conformations passing a steric filter, a physics-based scoring function was used to evaluate the fit to the binding site. For the best scoring conformation of each docked molecule, 100 steps of rigid-body minimization were carried out. The score for each conformation was calculated as the sum of the receptor–ligand electrostatic and van der Waals interaction energy, corrected for ligand desolvation. These three terms were evaluated from pre-calculated grids. The three-dimensional map of the electrostatic potential in the binding site was prepared using the program Delphi[4]. In this calculation, partial charges from the united atom AMBER force field[5] were used for all receptor atoms except the side chain hydroxyl of Tyr146$^{3.29}$ for which the dipole moment was

increased in screens of both fragment and lead-like libraries as described previously[6,7]. Additionally, in the screen of lead-like compounds, which extended further towards the extracellular regions of the orthosteric site, the dipole moments for side chain hydroxyls of Tyr347$^{7.31}$ and Thr226$^{5.27}$ and the backbone of Leu55$^{1.23}$ were also increased. The program CHEMGRID was used to generate a van der Waals grid based on a united atom version of the AMBER force field[5]. The desolvation penalty for a ligand conformation was estimated from a pre-calculated transfer free energy of the molecule between solvents of dielectrics 78 and 2. The desolvation energy was obtained by weighting the transfer free energy with a scaling factor that reflects the degree of burial of the ligand in the receptor binding site[8].

In the prospective screens, subsets from the ZINC database[9] of commercially available compounds were used. The fragment (molecular weight $\leq$ 250, LogP $\leq$ 3.5, and rotatable bonds $\leq$ 5) and lead-like (250 < molecular weight $\leq$ 350, LogP $\leq$ 3.5, and rotatable bonds $\leq$ 7) libraries contained 0.5 and 1.8 million unique compounds, respectively. All docked compounds were prepared for docking using the ZINC database protocol[9].

Similarity calculations. Similarity calculations for the discovered ligands were performed using the Screenmd program from Chemaxon[10]. The Tanimoto coefficient (T_c) with ECFP4 fingerprints for each ligand was calculated to all compounds from the ChEMBL21 database[11] that had been tested experimentally against NTSR1. Sub- and superstructure searches for identified ligands in commercial chemical libraries were performed using RDkit (www.rdkit.org).

Cloning of GPCR expression construct. The rat NTSR1 variant NTSR1-H4 was expressed in *E. coli* using a derivative of the vector pRG/III-hsMBP (kindly provided by R. Grisshammer (National Institute of Neurological Disorders and Stroke, National Institutes of Health, Rockville, MD, USA). NTSR1-H4 was N-terminally truncated at amino acid E44 (sequential NTSR1 numbering) and linked via a human rhinovirus (HRV) 3C protease site to a hexa-histidine tag and maltose-binding protein (MBP). At the C-terminus the receptor was truncated at amino acid G390 and fused via a hexa-glycine-serine linker to an Avi-tag, followed by a HRV 3C protease site, a penta-asparagine and a di-glycine-serine linker to thioredoxin A (TrxA) and a deca-histidine tag. Amino acids E273-T290 of the intracellular loop 3 were deleted and the two potential free cysteines C386 and C388 at the C-terminus of the receptor were both mutated to alanine. Truncations and removal of cysteine residues were carried out to facilitate protein purification, protein crystallization and biophysical experiments without perturbing signaling functionality of NTSR1-H4[2].

Protein expression. *Escherichia coli* BL21 cells were transformed with the expression plasmid encoding NTSR1-H4 and grown overnight at 37°C in 1 l of 2YT medium supplemented with 1% (w/v) glucose and 100 µg/mL ampicillin. A fermenter (Bioengineering D 558) containing 50 l of 2YT medium, 0.5% (w/v) glucose, and 100 µg/ml ampicillin was inoculated using the entire pre-culture and grown to an OD_{600} of 2.5 at 37°C. Receptor expression was induced with 1 mM isopropyl-β-D-thiogalactopyranoside (IPTG) and cells were cultivated at 28°C overnight. In addition, 1 µM biotin was added after induction to ensure efficient *in vivo* biotinylation of expressed NTSR1-H4 at the C-terminal Avi-tag. Cells were harvested

after overnight expression and cell pellets were frozen in liquid nitrogen and stored at -80°C.

Protein purification. For purification 25 g of frozen *E. coli* pellet were used. Cells were thawed at room temperature and resuspended in 50 ml of solubilization buffer, containing 100 mM HEPES pH 8.0, 20% (v/v) glycerol and 400 mM NaCl. All following steps were carried out at 4°C. 0.5 mL of 1 M $MgCl_2$ (5 mM), 2 mg DNase I, 200 mg lysozyme, and 20 ml of a detergent mixture composed of 0.2% (w/v) cholesteryl hemisuccinate Tris salt (CHS) and 2% (w/v) dodecyl-β-D-maltopyranoside (DDM) were added to the resuspended cell pellet. The mixture was incubated for 30 min, followed by cell lysis via mild sonification for 30 min in an ice-water bath. After cell lysis, 0.4 ml of 5 M imidazole was added and the mixture was incubated for another 30 min. The suspension was centrifuged for 30 min at 28,000 rcf. The supernatant was mixed with 5 ml of TALON resin (Clontech, Mountain View, CA, USA), which had been pre-equilibrated with IMAC binding buffer (25 mM HEPES pH 8.0, 10% (v/v) glycerol, 600 mM NaCl, 0.3% (w/v) DDM and 15 mM imidazole) and incubated for 2 h on a rolling device. Subsequently, the mixture was loaded into an empty PD10 column (GE Healthcare, Uppsala, Sweden) and was washed with 50 ml of IMAC binding buffer. Elution of bound protein was performed with 15 ml IMAC elution buffer containing 25 mM Hepes pH 8.0, 10% (v/v) glycerol, 150 mM NaCl, 0.3% (w/v) DDM and 250 mM imidazole. 500 µl of 1.6 mg/mL HRV 3C protease were added to the elution and incubated for 1 h at 4°C, followed by addition of 250 µl 10% (w/v) L-MNG and incubation for 1 h at 4°C. The cleaved protein was diluted threefold with SP binding buffer (10 mM HEPES pH 7.0, 10% (v/v) glycerol, and 0.01% (w/v) L-MNG) and was loaded onto a PD10 column containing 2.5 ml SP Sepharose beads pre-equilibrated with SP binding buffer. The

resin was washed with 15 ml SP binding buffer, followed by 12.5 ml of SP wash buffer (10 mM HEPES pH 7.7, 10% (v/v) glycerol, 35 mM NaCl, and 0.01% (w/v) L-MNG) and 2 mL SP binding buffer. NTSR1-H4 was eluted with 12 mL SP elution buffer (10 mM HEPES pH 7, 10% (v/v) glycerol, 350 mM NaCl, and 0.01% (w/v) L-MNG). Eluted receptor was concentrated in an Amicon-15 Ultra concentrator with a 50 kDa cutoff (Millipore, Billerica, MA, USA) to a final volume of less than 1 ml. Concentrated NTSR1-H4 was subjected to preparative size exclusion chromatography using a Superdex 200 10/300 GL column (GE Healthcare, Uppsala, Sweden), which had been pre-equilibrated with 10 mM HEPES pH 8, 150 mM NaCl, and 0.01% (w/v) L-MNG. Peak fractions corresponding to NTSR1-H4 were pooled (final volume 3-4 ml) and concentrated in an Amicon-4 Ultra concentrator with a 50 kDa cutoff to a final protein concentration of approximately 50 µM. Purified and concentrated NTSR1-H4 was mixed with 10 mM HEPES pH 8, 150 mM NaCl, 0.01% (w/v) L-MNG, and 50% (v/v) glycerol to yield a final glycerol concentration of 25%. Aliquots of 10 µl were frozen in liquid nitrogen and stored at -80°C for later usage.

SPR screening. All Surface Plasmon Resonance (SPR) measurements were performed on a Biacore T100 instrument (GE Healthcare) at 20°C. The receptor was immobilized via the in vivo biotinylated C-terminal Avi-tag on SAD500l sensor chips (XanTec, Düsseldorf, Germany) in running buffer (50 mM Tris pH 7.4, 150 mM NaCl, 0.1% (w/v) DDM, 2% DMSO) achieving 4000-5000 RU. Remaining free streptavidin sites were blocked by two 5 min injections of 2 µM amine-PEG_2-biotin (Thermo Scientific, Waltham, MA, USA). NTSR1 integrity and binding activity after coupling was verified by injections of a mutated NTS8-13 peptide comprising two alanine mutations at position 11 and 12, with previously determined binding

characteristics (E. Huber et al., submitted). All fragment- and lead-like compounds screened were purchased from Enamine, Chembridge, VitasM or Chemdiv (Supplementary Table 1). The purities of all discovered ligands were found to be ≥ 95% as judged by LC/MS or NMR. Analytes were initially screened at concentrations of 50 μM and 500 μM for leads and fragments, respectively. Screening was performed against immobilized free receptor (non-ligand bound) and blocked receptor, as well as a blank reference surface. Blocking of the orthosteric NTSR1 binding site was achieved by injection of 200 nM NTS8-13, which shows a remarkably slow off-rate when bound to NTSR1. All analytes were measured in duplicates. Ligand association was monitored over 60 s and dissociation over 300 s at a flow rate of 30 μl/min. Measurements were double-referenced and processed in Scrubber 2 software (BioLogic software, Campbell, Australia). Eighteen compounds were further evaluated in dose-response experiments at 8 concentrations ranging from 90-0.0123 μM for the leads and 270-0.041 μM for the fragments. Analogs of compounds **2**, **3**, and **34** were further evaluated at 8 concentrations ranging from 90-0.014 μM on the free and blocked receptor surface. To directly demonstrate saturation, we also plotted the plateau levels as a function of analyte concentration.

Functional assays. For functional assays, HEK293 cells stably expressing rat NTSR1 wild-type were produced using the HEK293 T-Rex Flp-In cell system (ThermoFisher Scientific, Waltham, MA, USA). Cells were cultured in Dulbecco's Modified Eagle Medium (DMEM) supplemented with tetracycline-free 10% fetal calf serum (FCS). NTSR1 expression was induced by addition of 1 μg/ml tetracycline to the medium. After 24 h, cells were harvested and signaling activity was measured in 384-well plates with competitive homogeneous time-resolved fluorescence (HTRF) assays for

cyclic AMP and inositol-1 phosphate (IP1) (a metabolite of inositol trisphosphate, IP3), using the cAMP Dynamic 2 and the IP-One TB assay kits (Cisbio, Codolet, France) according to the manufacturer's instructions.

Table S1. Structures (smiles) and purchasing information for all compounds evaluated experimentally.

ID	Compound SMILES	ZINC ID	Vendor
1	CC(C)C[CH](C(=O)[O-])NC(=O)NCc1ccccc1Cl	C02402950	VitasM
2	COC(=O)Nc1cccc(c1)NC(=O)C[CH](c2ccccc2)C(=O)[O-]	C55150343	Enamine
3	c1ccc(cc1)[CH](CC(=O)Nc2ccc(c(c2F)F)F)C(=O)[O-]	C13253230	Enamine
4	C[CH](c1ccc(cc1)OC)C(=O)NC[CH](c2ccccc2)C(=O)[O-]	C89904839	Enamine
5	c1cc(cc(c1)C(=O)N[CH](Cc2ccncc2)C(=O)[O-])Cn3cccn3	C95374199	Chembridge
6	c1c2n(nc1CCC(=O)[O-])CCCN(C2)C(=O)CCc3nc([nH]n3)N	C72408499	Chembridge
7	Cn1cccc1CCC(=O)N2CCCn3c(cc(n3)CCC(=O)[O-])C2	C72430998	Chembridge
8	Cc1cc(C(=O)N[CH](C)c2nnn[nH]2)c2ccc(C)c(C)c2n1	C77504963	Chembridge
9	C[CH](c1[n-]nnn1)NC(=O)c2cccc(c2)c3ccccc3F	C65428588	Chembridge
10	CCc1nc(c(o1)C(=O)N2CCCn3c(cc(n3)CCC(=O)[O-])C2)C	C72423431	Chembridge
11	Cc1c(c(n[nH]1)C)Cc2nnc(n2c3cccnc3)SCC(=O)[O-]	C67723243	Chembridge
12	C=CCc1cc(-c2cn([CH](C)c3nnn[nH]3)nn2)ccc1OC	C91624795	Chembridge
13	Cc1ccc(cc1N2CCNC2=O)C(=O)N[CH](C)c3[n-]nnn3	C91665087	Chembridge
14	CCOc1ccc(cc1)Cc2nnc(n2C)S[CH](C)C(=O)[O-]	C20462977	Chemdiv
15	CC(C)c1ccc(cc1)NC(=O)[CH](Cc2cccs2)c3[n-]nnn3	C05498617	Chemdiv
16	C[CH](C(=O)[O-])N(C)C(=O)OCC1c2ccccc2-c3c1cccc3	C00057598	Enamine
17	c1ccc(c(c1)C(=O)[O-])OCc2cc(on2)c3ccco3	C37207738	Enamine
18	CCC[CH](c1[n-]nnn1)NC(=O)c2csc(n2)Cc3ccccc3	C75107656	Enamine
19	c1cc(cc(c1)F)c2nc(cs2)CC(=O)NCC3(CCC3)C(=O)[O-]	C89779396	Enamine
20	c1ccc2c(c1)-c3ccccc3C2COC(=O)NCCC(=O)[O-]	C02169812	Enamine
21	c1ccc(cc1)CN(CC(=O)Nc2[n-]nnn2)c3ccccc3	C95441256	Enamine
22	CC(C)C[CH](C(=O)[O-])NC(=O)c1cn(nn1)Cc2ccccc2	C95427717	Enamine
23	CC(C)C[CH](C(=O)[O-])NC(=O)OCC1c2ccccc2-c3c1cccc3	C01541051	Enamine
24	c1ccc(c(c1)CNc2ccc3nnc(n3n2)CCC(=O)[O-])Cl	C13366081	VitasM
25	CC(C)C[CH](C(=O)[O-])NC(=O)N1CCN(CC1)c2ccccc2	C00539688	VitasM
26	C[CH](C(=O)[O-])NC(=O)N1CCN(CC1)c2c3ccccc3sn2	C72402163	VitasM
27	C[CH](C(=O)[O-])NC(=O)N1CCC(CC1)Cc2ccccc2	C05277622	VitasM
28	Cc1ccc(o1)C(=O)NCc2c(cco2)C(=O)[O-]	C00248333	Chembridge
29	CC(C)[CH](C(=O)[O-])NC(=O)NC1CCCCC1	C00546828	Enamine
30	c1ccc(cc1)C(=O)N2CCC[CH]2C(=O)[O-]	C06595049	VitasM
31	CCc1ccccc1NC(=O)N[CH](C)C(=O)[O-]	C00535074	VitasM
32	C[CH](C(=O)[O-])NC(=O)c1cc2c(s1)CCC2	C19274765	Enamine
33	C[CH](C(=O)[O-])NC(=O)N1CCc2c1cccc2	C13691930	VitasM
34	c1ccc(cc1)C(=O)N[CH](c2[n-]nnn2)C3CC3	C68575838	Enamine
35	CC(C)(C(=O)[O-])NC(=O)c1ccc2c(c1)cc[nH]2	C95394010	Enamine
36	c1cc2c(cc1Cl)c(=O)c(co2)/C=C/C(=O)[O-]	C00096003	VitasM
37	c1cc(sc1)c2c(cn(n2)CCC#N)C(=O)[O-]	C03355986	Enamine
38	C[CH](C(=O)[O-])NC(=O)N1C[CH]2CC[CH]1C2	C49724433	Enamine
39	C[CH](C(=O)[O-])NC(=O)CC1CCCCC1	C20250200	Enamine

40	Cn1cc(c(n1)c2ccc(cc2F)F)C(=O)[O-]	C36894477	Enamine
41	CCCc1cc([nH]n1)C(=O)N[CH](C)c2[n-]nnn2	C91320028	Chembridge
42	CCOC(=O)C[P](=O)(c1ccccc1)[O-]	C22343250	Chembridge
43	C[CH](C(=O)[O-])NC(=O)Cn1ccc2c1cccc2	C36369994	Chembridge
44	c1ccc(c(c1)n2cnnc2Cc3[n-]nnn3)F	C67642361	Chembridge
45	CCCc1c(cn(n1)Cc2ccccc2)C(=O)[O-]	C32627631	Enamine
46	C[CH]1C[CH]1C(=O)Nc2ccc(cc2C(=O)[O-])F	C19423812	Enamine
47	Cc1ccc2c(c1)[nH]c(n2)SCc3[n-]nnn3	C75572290	Enamine
48	c1ccc(cc1)/C=C(/c2ccccc2)\C(=O)[O-]	C00080749	Enamine
49	c1ccc2c(c1)ccc(n2)SCCC(=O)[O-]	C06146180	VitasM
50	CN(C[P](=O)(CCc1ccccc1)[O-])C=O	C00066432	VitasM
51	c1ccc2c(c1)CCN(C2)C(=O)CCC(=O)[O-]	C03634359	VitasM
52	C[CH](C(=O)[O-])NC(=O)c1ccc(cc1)F	C00146181	VitasM
53	CCC[CH](c1[n-]nnn1)NC(=O)c2cc(cc(c2)F)C	C95965248	Enamine
54	CCC[CH](c1[n-]nnn1)NC(=O)c2cc(ccc2C)C	C89949627	Enamine
55	CCC[CH](c1[n-]nnn1)NC(=O)c2ccc(cc2C)OC	C84740434	Enamine
56	CCC[CH](c1[n-]nnn1)NC(=O)c2cc(c(cc2F)F)C	C89949619	Enamine
57	CCC[CH](c1[n-]nnn1)NC(=O)c2ccc(cc2F)OC	C89949671	Enamine
58	CCC[CH](c1[n-]nnn1)NC(=O)c2ccc(cc2C)C	C89949667	Enamine
59	CCC[CH](c1[n-]nnn1)NC(=O)c2ccccc2OC	C95287819	Enamine
60	CCC[CH](c1[n-]nnn1)NC(=O)c2cc(cnc2)Br	C84740425	Enamine
61	CCC[CH](c1[n-]nnn1)NC(=O)c2cc(ccc2O)C	C92424876	Enamine
62	CCC[CH](c1[n-]nnn1)NC(=O)c2cc(c(cc2Cl)F)F	C89949615	Enamine
63	CCC[CH](c1[n-]nnn1)NC(=O)c2cccc(c2)n3cccn3	C89949685	Enamine
64	CCC[CH](c1[n-]nnn1)NC(=O)c2cc(ccn2)n3cccn3	C89949631	Enamine
65	CCC[CH](c1[n-]nnn1)NC(=O)c2ccc3c(c2)CCC3	C95287795	Enamine
66	CCC[CH](c1[n-]nnn1)NC(=O)c2cc(cnc2)C	C89949641	Enamine
67	c1ccc(cc1)[CH](CC(=O)Nc2cccc(c2)Cl)C(=O)[O-]	C13250143	Enamine
68	c1ccc(cc1)[CH](CC(=O)Nc2ccccc2Cl)C(=O)[O-]	C04671131	Enamine
69	COc1ccccc1NC(=O)C[CH](c2ccccc2)C(=O)[O-]	C13249839	Enamine
70	CC(=O)Nc1ccc(c(c1)NC(=O)C[CH](c2ccccc2)C(=O)[O-])F	C44830413	Enamine
71	COc1cccc(c1)NC(=O)C[CH](c2ccc(cc2)F)C(=O)[O-]	C25204967	Enamine
72	c1ccc(cc1)[CH](CC(=O)Nc2ccc(cc2)O)C(=O)[O-]	C13469745	Enamine
73	CCOc1ccccc1NC(=O)C[CH](c2ccccc2)C(=O)[O-]	C13253669	Enamine
74	c1ccc(cc1)[CH](CC(=O)Nc2cccc(c2)Br)C(=O)[O-]	C12696622	Enamine
75	COc1ccc(cc1NC(=O)C[CH](c2ccccc2)C(=O)[O-])Cl	C13250265	Enamine
76	c1cc(c(c(c1NC(=O)[CH]2CCCC[CH]2C(=O)[O-])F)F)F	C31979653	Chembridge
77	c1cc(c(c(c1NC(=O)[CH]2CC=CC[CH]2C(=O)[O-])F)F)F	C12802409	Enamine

Table S2. Most similar compounds from the CHEMBL21 database that had been tested at NTSR1 to each ligand identified from the screen of a lead-like library along with 2D similarity (T_c) values.

ID	Ligand Structure	Closest compound	2D similarity (T_c)[a]
1	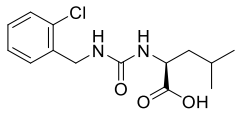	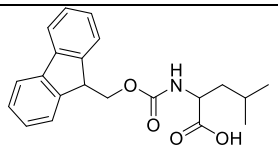	0.45
2	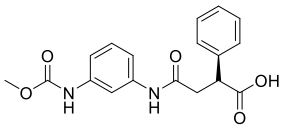	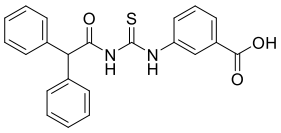	0.38
3	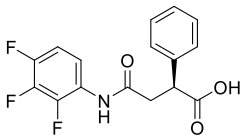	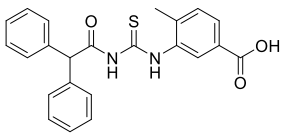	0.30
4	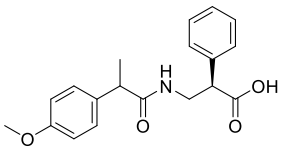	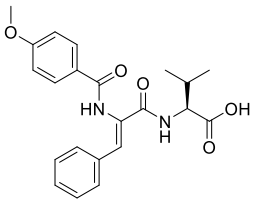	0.36
5	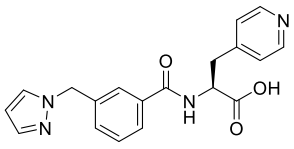	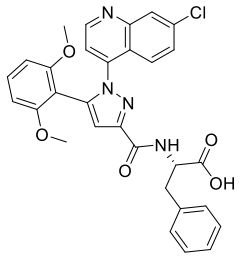	0.34

[a] The maximal Tanimoto coefficient (ECFP4) when compared with all the compounds tested at NTSR1 in the CHEMBL21 database.

Table S3. Most similar compound from the CHEMBL21 database that had been tested at NTSR1 to each ligand identified from the screen of the fragment library along with 2D similarity (T_c) values.

ID	Ligand structure	Closest compound	2D similarity (T_c)[a]
29	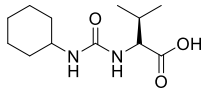	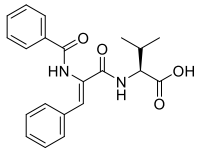	0.32
30	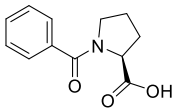	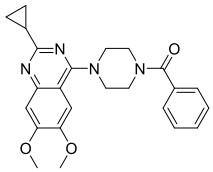	0.30
31	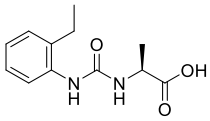	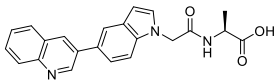	0.32
32	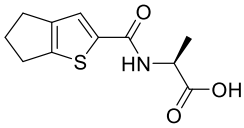	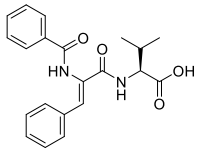	0.27
33	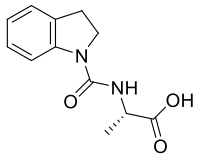	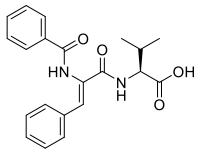	0.29
34	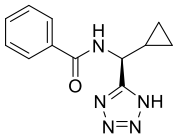	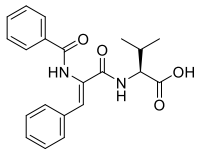	0.28
35	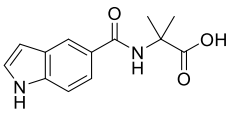	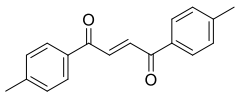	0.23
36	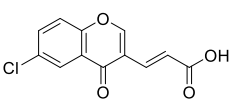	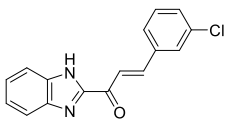	0.29

[a] The maximal Tanimoto coefficient (ECFP4) when compared with all the compounds tested at NTSR1 in the CHEMBL21 database.

Table S4. Experimental data for analogs of compound **34**.

ID	Ligand structure	$K_{D,kinetic}$ (μM)[a]	$K_{D,equilibrium}$ (μM)[b]	LE[c]
53	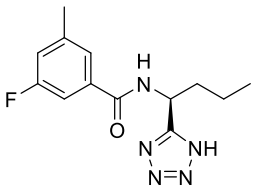	17.5	13.7	0.34
54	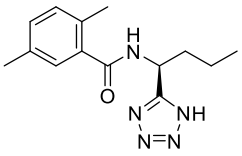	24	29.5	0.33
55	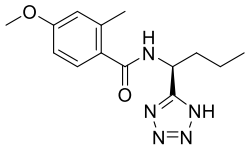	(15.9)[d]	(17.3)	(0.33)
56	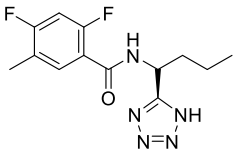	15.8	14.6	0.33
57	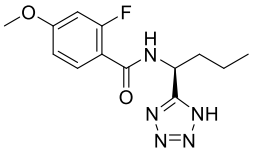	22.6	24	0.32
58	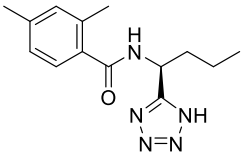	11.8	13.9	0.35
59	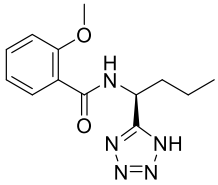	(31.3)	(22.4)	(0.32)
60	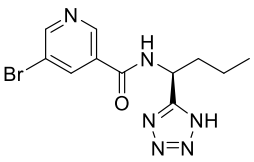	38.3	32.5	0.32

61	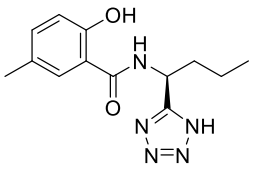	(46.6)	(19.7)	(0.29)
62	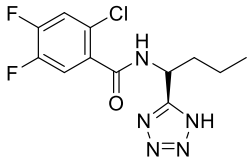	(380)	N.B.[e]	(0.26)
63	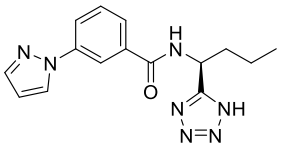	33.3	44.9	0.28
64	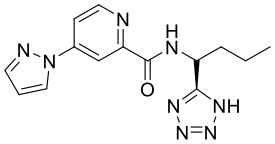	30.7	46.1	0.28
65	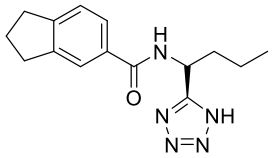	4.4	6.7	0.36
66	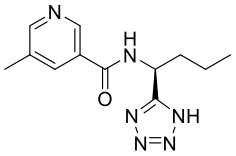	(33.7)	(54.8)	(0.34)

[a] K_D from kinetic analysis.
[b] K_D from equilibrium analysis.
[c] LE (kcal mol^{-1} $atom^{-1}$) calculated as $-RT\ln(K_{D,kinetic})/N$, where N is the number of heavy atoms.
[d] Values in parenthesis show signs of saturation, but very low RU values and/or high error bars.
[e] N.B., compound displayed no detectable binding.

Table S5. Experimental data for analogs of compounds **2** and **3**.

ID	Ligand Structure	$K_{D,kinetic}$ (μM)[a]	$K_{D,equilibrium}$ (μM)[b]	LE[c]
67	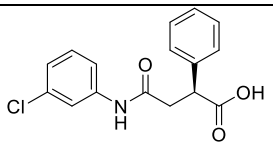	0.6	1.1	0.42
68	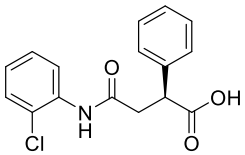	0.5	0.6	0.43
69	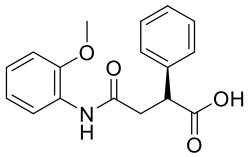	0.4	0.52	0.42
70	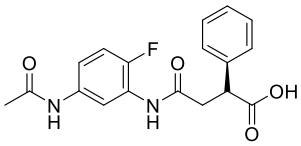	1	2.3	0.37
71	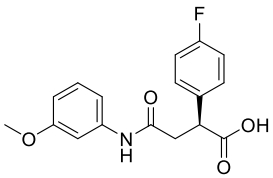	2.8	4.7	0.34
72	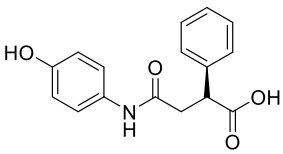	27.5	4.8	0.31
73	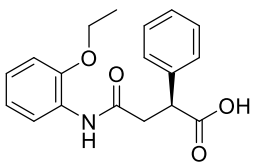	0.6	0.5	0.39
74	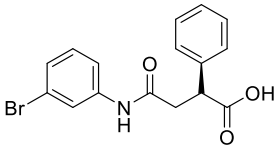	0.5	0.7	0.43

75	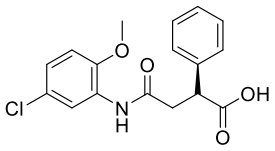	0.6	0.5	0.39
76	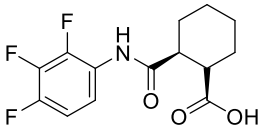	N.B.[d]	N.B.[d]	–
77	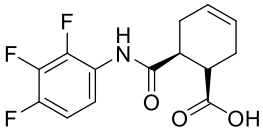	N.B.[d]	N.B.[d]	–

[a] K_D from kinetic analysis.
[b] K_D from equilibrium analysis.
[c] LE (kcal mol^{-1} $atom^{-1}$) calculated as $-RTln(K_{D,kinetic})/N$, where N is the number of heavy atoms.
[d] N.B., compound displayed no detectable binding.

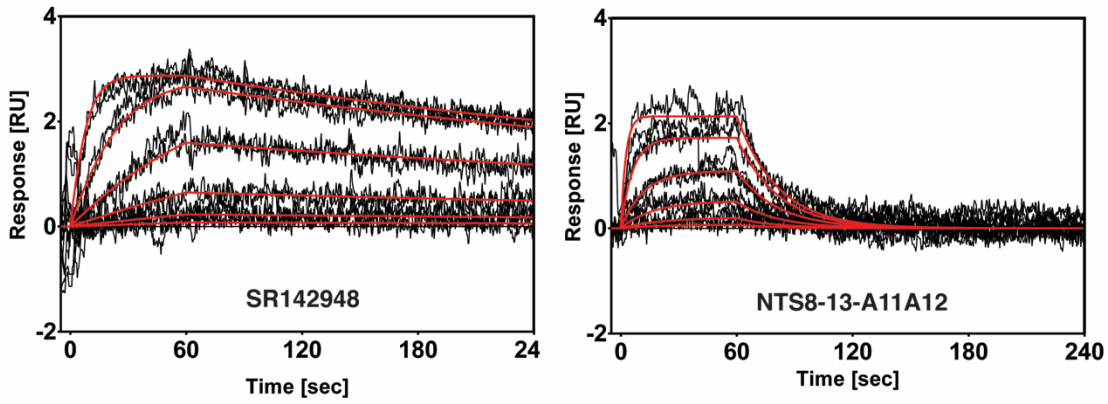

Figure S1. SPR analysis of NTSR1 ligands. SPR data for reference antagonist SR142948 and peptide agonist NTS8-13 with alanine mutations at position 11 and 12 (NTS8-13-A11A12). Red lines represent kinetic fits using a 1:1 binding model.

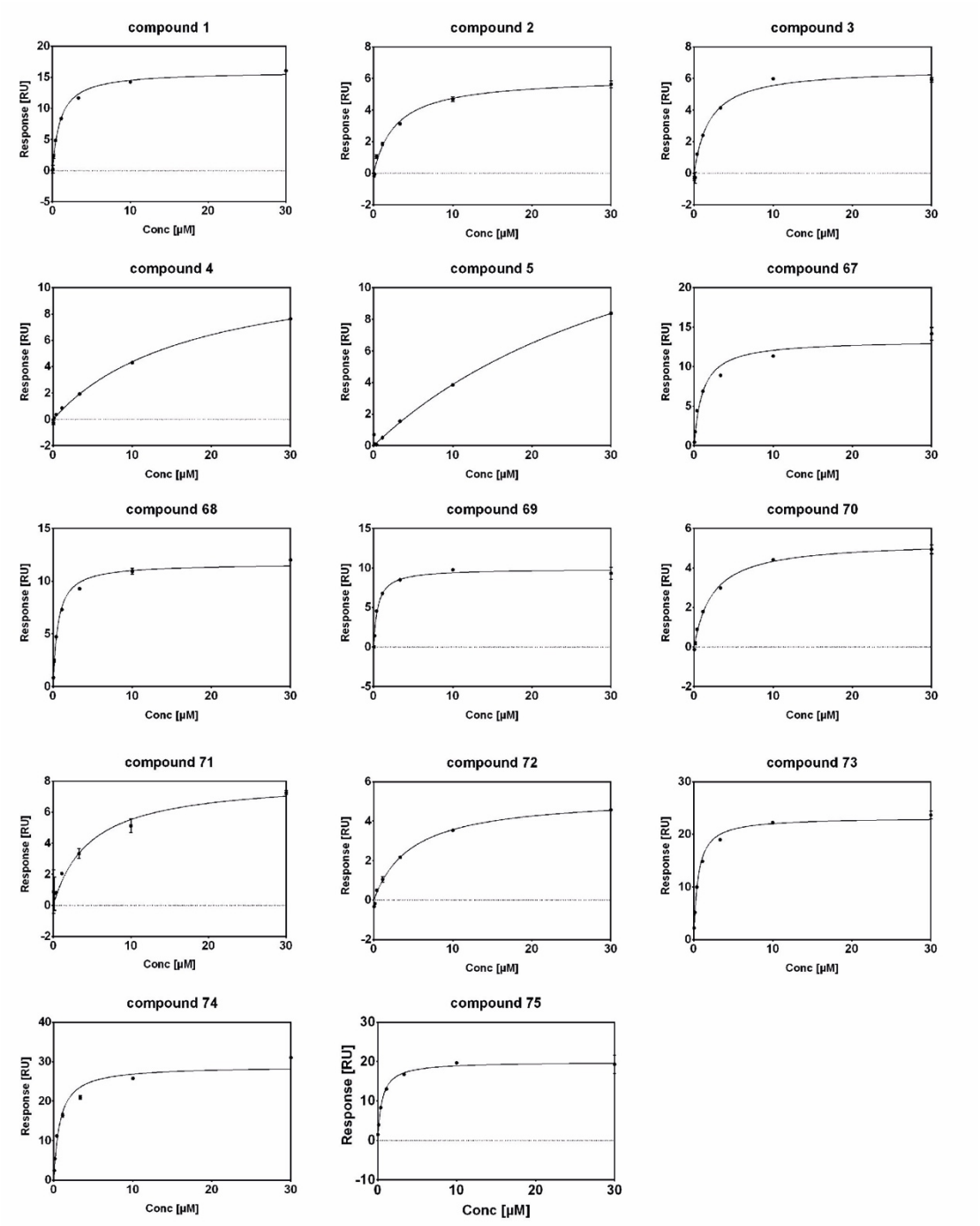

Figure S2. SPR analysis of compounds from the lead-like library. Equilibrium fits for compounds **1**-**5** and **67**-**75**.

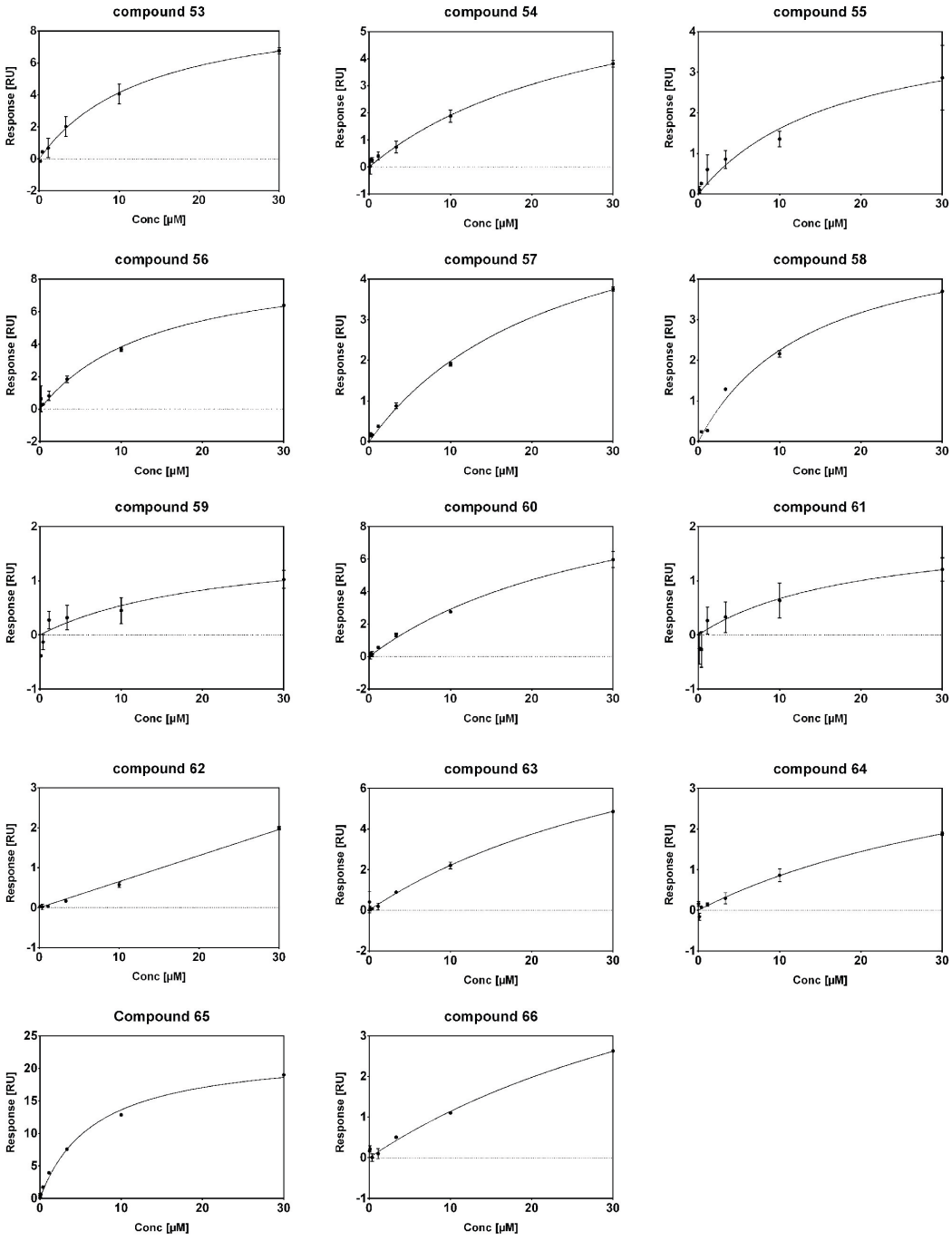

Figure S3. SPR analysis of analogs to compound 34. Equilibrium fits for compounds **53-66**.

Supporting references

(1) Lorber, D. M., and Shoichet, B. K. (2005) Hierarchical docking of databases of multiple ligand conformations, *Curr Top Med Chem 5*, 739-749.

(2) Egloff, P., Hillenbrand, M., Klenk, C., Batyuk, A., Heine, P., Balada, S., Schlinkmann, K. M., Scott, D. J., Schutz, M., and Plückthun, A. (2014) Structure of signaling-competent neurotensin receptor 1 obtained by directed evolution in Escherichia coli, *Proc Natl Acad Sci USA 111*, E655-E662.

(3) Shoichet, B. K., and Kuntz, I. D. (1993) Matching chemistry and shape in molecular docking, *Protein Eng 6*, 723-732.

(4) Nicholls, A., and Honig, B. (1991) A rapid finite difference algorithm, utilizing successive over-relaxation to solve the Poisson–Boltzmann equation, *J Comput Chem 12*, 435-445.

(5) Weiner, S. J., Kollman, P. A., Case, D. A., Singh, U. C., Ghio, C., Alagona, G., Profeta, S., and Weiner, P. (1984) A new force-field for molecular mechanical simulation of nucleic-ccids and proteins, *J Am Chem Soc 106*, 765-784.

(6) Carlsson, J., Yoo, L., Gao, Z.-G., Irwin, J. J., Shoichet, B. K., and Jacobson, K. A. (2010) Structure-based discovery of A_{2A} adenosine receptor ligands, *J Med Chem 53*, 3748-3755.

(7) Chen, D., Ranganathan, A., IJzerman, A. P., Siegal, G., and Carlsson, J. (2013) Complementarity between in silico and biophysical screening approaches in fragment-based lead discovery against the A_{2A} adenosine receptor, *J Chem Inf Model 53*, 2701-2714.

(8) Mysinger, M. M., and Shoichet, B. K. (2010) Rapid context-dependent ligand desolvation in molecular docking, *J Chem Inf Model 50*, 1561-1573.

(9) Irwin, J. J., and Shoichet, B. K. (2005) ZINC--a free database of commercially available compounds for virtual screening, *J Chem Inf Model 45*, 177-182.

(10) ChemAxon. (2012) JChem, version 5.11.4, Budapest.

(11) Gaulton, A., Bellis, L. J., Bento, A. P., Chambers, J., Davies, M., Hersey, A., Light, Y., McGlinchey, S., Michalovich, D., Al-Lazikani, B., and Overington, J. P. (2012) ChEMBL: a large-scale bioactivity database for drug discovery, *Nucleic Acids Res 40*, D1100-1107.